The Coupled Logistic Map

Justin Deterding
Dept. of Physic and Astronomy
University of New Mexico
jdeterding@unm.edu

Catherine Wright
Dept. of Computer Science
University of New Mexico
wrightc@unm.edu

***Abstract*—This project provides a thorough in-depth analysis of a paper that suggests the transition from bottom-up to top-down causal information transfer in biological systems. We utilize a toy model simulating the dynamics of coupled logistic maps, finding both reassurances and discrepancies in the previous work. Our analysis works to expand and investigate on these past results by exploring the dynamics of the system with a reproductive rate coupled to the global population.**

I. Introduction

In molecular biology the central dogma suggest a bottom-up flow of information in biological systems. That information comes from the DNA, however information does not flow from the system to the DNA. In many other reductionist sciences the idea persists that once we fully understand the fundamental components of a system then the entire evolution of the system can be understood. This previous understanding led to the belief that information transfer comes from the bottom up, making it so once we understand these fundamental components we then can understand the whole. This concept was recently challenged in [1], which we will refer to as the Walker paper. In this project we review parts of the Walker paper, attempting to recreate some of the previous results while also expanding on their analysis while investigating some of the ideas further. We beginning by reviewing basic measures of Shannon entropy and mutual information. After, we replicated the toy model used in the Walker paper for examining collective behavior in a globally coupled chaotic system. We delve deeper into the transfer entropy of different coupling rates and compare our results with those discovered in the Walker paper. To develop further understanding of coupled chaotic behaviors we then review the dynamics of a system with an alternate form of coupling of individuals to the global population. The project finishes with a brief discussion and conclusion of our results.

II. Methods and Results

A. Shannon Entropy and Mutual Information

To begin, we start by measuring the entropy levels and mutual information levels for a non-chaotic and chaotic time series. In figure 1 there are two sets of two time series. Each set of time series has two individual time series both with the same reproduction fitness coefficient, but slightly different initial populations. The coefficients were selected such that one series displays a chaotic behavior ($r = 3.7$), while the other displayed non-chaotic behavior ($r = 2.9$). For each

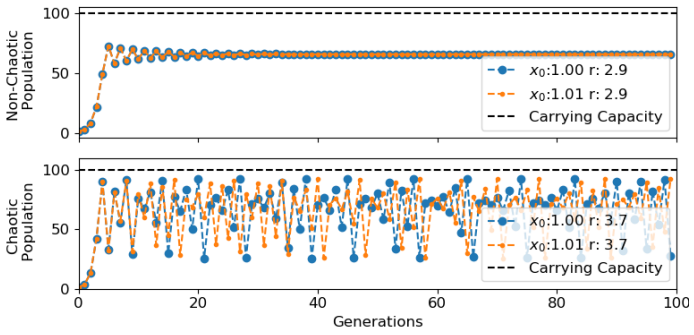

Fig. 1. Time series of a non-chaotic population (top set) and chaotic population (bottom set) Reproductive coefficients (2.9,3.7) are equal for each series in a set. Initial populations are varied in each set (1.00,1.01).

time series in either set the initial population was varied by 1% of the other, as seen in the legends of the plots (x_0 variable). The non-chaotic time series track closely together for all generations and eventually reach equal steady state populations. The chaotic series track each other for the first 15 generations before diverging significantly. In figure 2 the Venn diagrams illustrate the scale of the Shannon entropy ($H(X)$, $H(Y)$) of each time series and the mutual information ($I(X,Y)$) in each time series for the first 15 generation and the last 15 generations. The entropy and mutual information measures were done using the JIDT tool [4]. For all measures the binned method of measurement was used with data discretized into 10 bins. The diameter of the individual circles is scaled to the entropy measure, and distance overlapping is scaled to the mutual information measure. In this way, if the individual entropy measures both equal the mutual information measure, then both circles overlap (figure 2, "First 15 Non-Chaotic") and if there is no mutual information, then there is no overlap. The circles appear as ovals, rather than circles for some figures. This is a because of auto-fitting in the Python Matplotlib library. At this point it was not worth the time to attempt to scale it correctly, what is of primary concern is the horizontal overlap. For the first 15 generations the non-chaotic series track each other very closely, and merge closer together with increasing generations. It should be noted that the diagrams should be slightly different is size, however the variation it the two series is too small to capture given the level of data discretization. As a result, they share mutual information equivalent to their individual entropy measures

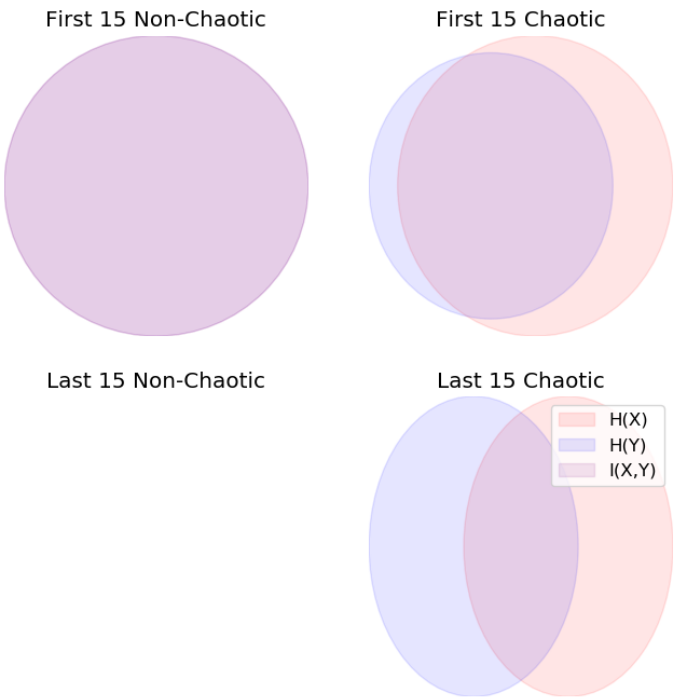

Fig. 2. Venn diagrams illustrating the relative scale of the entropies, and the mutual information measures for the first and last 15 generations. *NOTE: the last 15 Non-Chaotic is not missing. The entropies are zero therefore there are no diagrams*

(2.0419 bits). In the first 15 generations of the chaotic time series we note that the mutual information is quite high (2.3899 bits) however there is difference in the individual entropies (3.0566 bits and 2.7069 bits), and that they don't completely overlap is because they are beginning to diverge with each increasing generation. For the final 15 time steps, the non-chaotic series have converged to the same value. The diagram is empty because the entropy measures and therefore the mutual information are both zero. There is no change, no information, and no information that could be mutual. For the chaotic series, they have identical measures of entropy (both 2.6891 bits), with some mutual information (1.4716 bits).

B. Replication of Walker's Toy Model

In [1], Walker simulates a toy model that portrays the non-trivial collective behavior in a globally coupled chaotic map lattice. This collective behavior is used to look into the causal structure of differently coupled populations in attempt to show how the top-down informational flow can lead to the emergence of a higher-level entity. The toy model is a variation of the discrete logistic growth model that incorporates the mean-field of the meta-population and weights the individual and the mean-field (m_n, defined in (4)) by a coupling coefficient. The model is defined below for i and n denoting a single population and a single generation respectively.

$$x_{i,n+1} = (1-\epsilon)f_i(x_{i,n}) + \epsilon m_n \;\; ; \;\; (i = 1, 2, \ldots N) \tag{1}$$

The global coupling strength (ϵ) is the weighting constant that determines the connection between individual behavior and the total population. The function $f_i(x_{i,n})$, as shown in (2), calculates the local dynamics according to the logistic map of population i at generation n. In this equation r_i represents the reproductive fitness of population i. Since this is a model of the collective behavior in coupled chaotic systems, the reproductive fitness value is always in the chaotic regime. The carrying capacity (K), also defined as the maximum population size, was set to $K = 100$ to match [1].

$$f_i(x_{i,n}) = r_i x_{i,n}\left(1 - \frac{x_{i,n}}{K}\right) \tag{2}$$

At a given generation n, the instantaneous state of the meta-population (M_n) is calculated by the average of all local populations, shown as

$$M_n = \frac{1}{N}\sum_{j=1}^{N} x_{j,n} \tag{3}$$

which is referred to as the instantaneous mean-field. To evaluate the dynamics at a particular mean-field we can take the average of $f_j(x_{j,n})$ for all populations.

$$m_n = \frac{1}{N}\sum_{j=1}^{N} f_j(x_{j,n}) \tag{4}$$

Walker defines the instantaneous dynamics of the mean-field as a "global systemic entity", meaning that it acts as a superorganism with collective intelligence that cannot be linked to a single individual in the population, but rather to the complex collective behavior of the whole. Below is a quote from Mitchell [2] that inspires why we evaluate this behavior.

> "It is the collective actions of vast numbers of components that give rise to the complex, hard-to-predict, and changing patterns of behavior that fascinate us." (p. 12)

In simulating the toy model we chose to replicate the parameters Walker used. As mentioned, carrying capacity was set to $K = 100$, simulating $N = 1,000$ populations over the course of $10,000$ generations. For every population we initialized $x_{i,0} = 1$, and r_i was drawn independently and uniformly from the interval [3.9, 4.0]. Figure 3 shows the return map comparing the mean fields for global coupling strength $\epsilon \in [0, 0.075, 0.1, 0.2, 0.225, 0.25, 0.3, 0.4]$ and a single logistic map. It should be noted that this is a stochastic system. The randomness provided by varying values of r_i produce very different looking return maps each time the simulation is run. Being said, the qualitative behavior of the return maps is consistent, typically maintaining the same shapes for different values of ϵ.

To interpret what the return map shows we can first think of the two extreme values of the global coupling strength. For $\epsilon = 0$ each value of $x_{i,n+1}$ is calculated by $x_{i,n+1} = f_i(x_{i,n})$, meaning each sub-population is an independent entity with its behavior not driven by the meta-population's dynamics. On the other side of the spectrum $\epsilon = 1$ produces $x_{i,n+1} = m_n$,

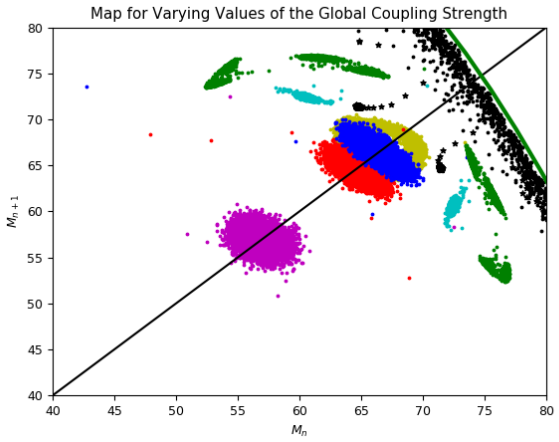

Fig. 3. Return map for different global coupling strengths: $\epsilon = 0$ (magenta), $\epsilon = 0.075$ (red), $\epsilon = 0.1$ (blue), $\epsilon = 0.2$ (yellow), $\epsilon = 0.225$ (cyan), $\epsilon = 0.25$ (dark green), $\epsilon = 0.3$ (black stars), and $\epsilon = 0.4$ (black). A single logistic map is shown in green.

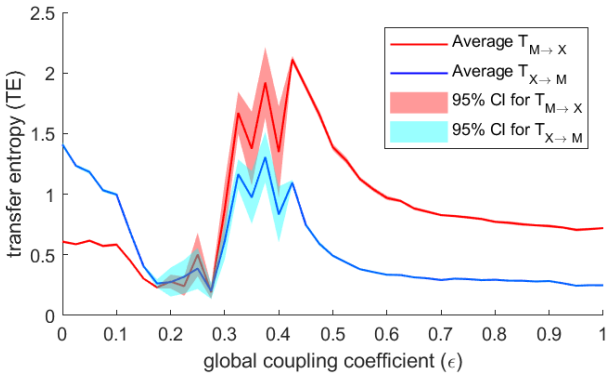

Fig. 4. Averages and 95% confidence intervals (CI) of top-down ($T_{M\to X}$ in red) and bottom-up ($T_{X\to M}$ in blue) causal information transfer displayed as a function of the global coupling strength ϵ

meaning that each population at every generation is strictly following the dynamics of the mean-field, completely coupling the sub-populations. Between these two extremes the sub-populations experience clustering patterns similar to the periodic motion in dynamical systems. The uncoupled return map (figure 3, magenta) shows the independent populations dispersed around a fixed point. Where our results differ from [1] is in the collective behavior of $\epsilon = 0.075$ (figure 3, red). The return map in [1] displayed a quasi-periodic three state oscillatory dynamic, where as ours did not demonstrate this collective sub-communal pattern until $\epsilon = 0.225$. For high coupling strength, as in $\epsilon = 0.4$ (figure 3 black), behavior is strongly coupled to the mean-field making the return map mimic the chaotic attractor [5], following the arch of a single logistic map (figure 3, green). These results are discussed further in section II-C where they can be compared to both top-down and bottom-up transfer entropy.

C. Information Transfer: Evaluating Bottom-Up and Top-Down Perspectives

Walker works to show that there is both top-down as well as bottom-up informational transfer between levels of organization that lead to the emergence of more complex biological organisms. To show quantitative results for this statement we can utilize transfer entropy, which measures the amount of information exchanged from one system to another [3]. The equation for the transfer entropy measured in bits from system Y to system X is

$$T^{(k)}_{Y\to X} = \sum_n p(x_{n+1}, x^{(k)}_n, y^{(k)}_n) log\left[\frac{p(x_{n+1}|x^{(k)}_n, y^{(k)}_n)}{p(x_{n+1}|x^{(k)}_n}\right] \quad (5)$$

such that k is the dimension of embedding, where similar to the order of a Markov process, k signifies how many generations previous are used to calculate the information transferred for a given generation. In [1], Walker uses many different values of k, choosing $T_{Y\to X} = Max\{T^{(k)}_{Y\to X}\}$. Due to issues in Java heap space using MatLab our simulation could not calculate transfer entropy for $k \geq 3$, so our results are found taking the maximum transfer entropy of $k = 1$ and $k = 2$. To perform this analysis we utilized the toy model described in II-B to simulate 10 meta-populations with each containing 1,000 sub-populations simulated over 1,000 generations. As before, carrying capacity was fixed at $K = 100$ with an initial population size $x_{i,0} = 1$. For each meta-population the instantaneous mean-field M was stored alongside 3 randomly chosen sub-populations. The JIDT tool [4] was used to generate MatLab code to calculate the transfer entropy from one vector to another. This resulted in 30 data points for each value of ϵ, such that ϵ ranged from 0 to 1 in increments of 0.025. The average transfer entropy for each global coupling parameter is shown in figure 4 with top-down causal information transfer shown in red and bottom-up transfer shown in blue, with 95% confidence bands around each average shaded in the corresponding colors.

Comparing the transfer entropy at varying global coupling strengths reveals a relation between dominant top-down information transfer and the formation of sub-communities in the return map shown in figure 3. For $0 \leq \epsilon < 0.2$ there is greater information transfer from the population to the mean-field, and the return map values in figure 3 show fixed-point behavior as populations act semi-independently. The level of uncertainty between $0.2 \leq \epsilon < 0.3$ makes it difficult to determine which direction of information transfer is highest, however it is in this range that communities start to emerge in the return map, suggesting an influence from the mean-field. For $\epsilon = 0.3$ the mean-field behavior acts near-periodic, and as the global coupling strength increases to $\epsilon = 0.4$ the mean-field begins behaving chaotically. For all $\epsilon > 0.3$ top-down causal information transfer is dominant.

To measure the mutual information between sub-populations sampled above we again utilized code produced by JIDT [4]. For each value of ϵ we calculated the mutual information of each pair of sub-populations within the 10

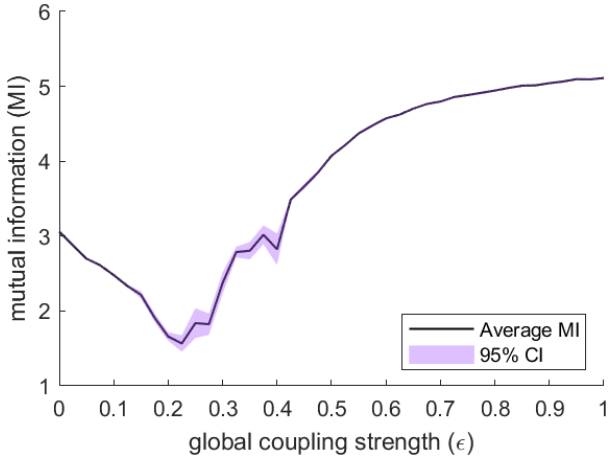

Fig. 5. Average mutual information (MI) measured in bits between sub-populations. 95% confidence interval showing uncertainty in MI.

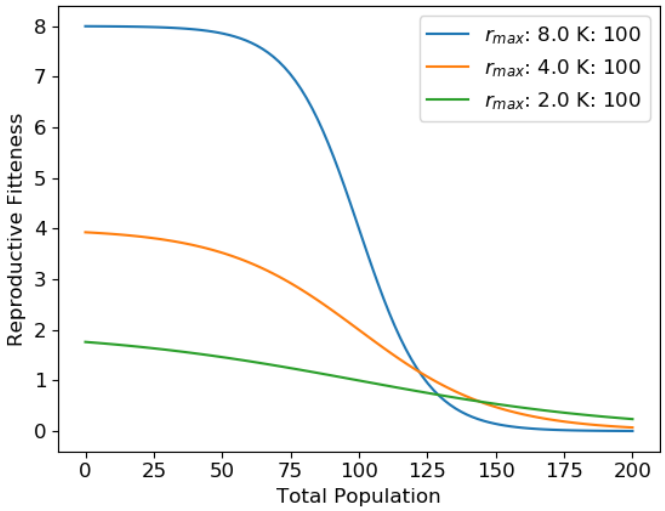

Fig. 6. Modified sigmoid function used to calculate the reproductive rate as a function of the total population.

meta-populations, i.e. a single meta-population produced 3 data points, $I(X_1, X_2)$, $I(X_2, X_3)$, and $I(X_1, X_3)$, for sub-populations X_1, X_2 and X_3. Figure 5 shows the average of this data with 95% confidence bands. The most uncertain range of sub-population mutual information coincides with the most uncertain range of transfer entropy. The minimum reached in mutual information seems to be at the point where the dominant direction of information flow changes from bottom-up to top-down. Since we do not see any of the behavior discovered in [1] at $\epsilon = 0.075$, neither in transfer entropy nor in mutual information, it does not seem to be the case that the quasi-periodic response seen in that work was caused by top-down information transfer.

D. Total Population Dependent Reproductive Rate

For the choose your own adventure we coupled the individual logistic equation together through the reproduction rate r_i. This was done by mapping the global population to a monotonically decreasing function. For this we used a modified version of the sigmoid function. We start with the basic logistic map equation.

$$x_{i,n+1} = r_i(x_{i,n})x_{i,n}(1 + \frac{x_{i,n}}{K}) \tag{6}$$

Where we then defined the reproduction coefficient to be

$$r_i(x_{i,n}) = \frac{r_{max}}{1 + e^{x_{norm}}} \tag{7}$$

such that the variable x_{norm} is defined as

$$x_{norm} = \Big(\sum x_i - K\Big)\frac{R_{max}}{K}. \tag{8}$$

The reproductive rate as a function of the total population is illustrated in figure 6 below. The key characteristics of this equation is that at low total populations, the reproductive rate is high, and for increasing total populations the reproductive rate decreases. This prevents the population from exploding. In exploring the dynamics of this system we begin by investigating the population dynamics for a system with a small

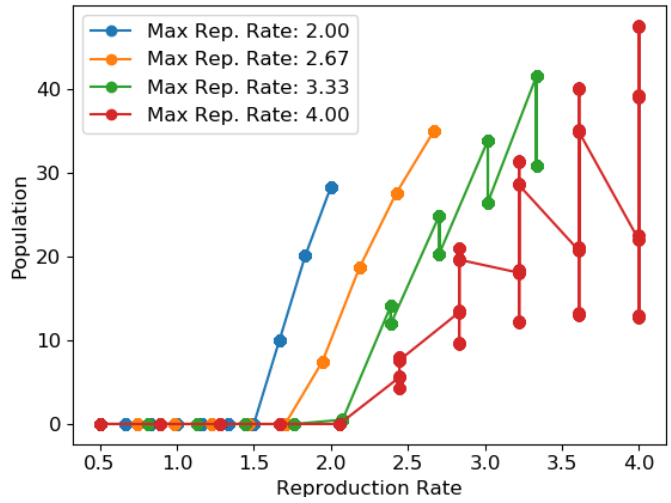

Fig. 7. Bifurcation map for small number of coupled populations. Each individual map has 10 sub-populations with increasingly larger maximum reproduction rates. We note that populations with small reproductive rates die out, and at high maximum reproductive rates we see branching of the steady state populations.

number of populations, then move to systems with a larger number of individual populations coupled together. We do this to gain some basic understanding of if the system reaches some steady state solution, and how the steady state solutions might vary with increased maximum reproductive rate. In figure 7 we have a bifurcation map. For all the series in this plot there are 10 individual populations, with linearly increasing reproduction coefficients from 0.5 to the specified maximum reproduction rate. There are several important take-aways from this plot. First, populations with a low reproductive rate die out. This is further illustrated in figure 8 for the reproductive coefficient of 1.44. Second, for low maximum reproduction rate the entire system merges to a single steady state solution similar the individual logistic map for small

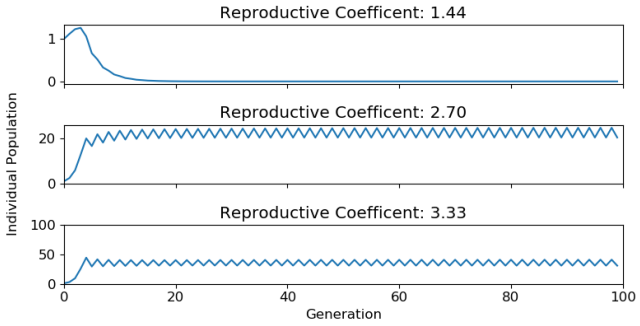

Fig. 8. Time series for individual populations in the bifurcation map above with maximum reproductive rate of 3.33 (red). Note that at this point the individual populations oscillate together between their stable populations.

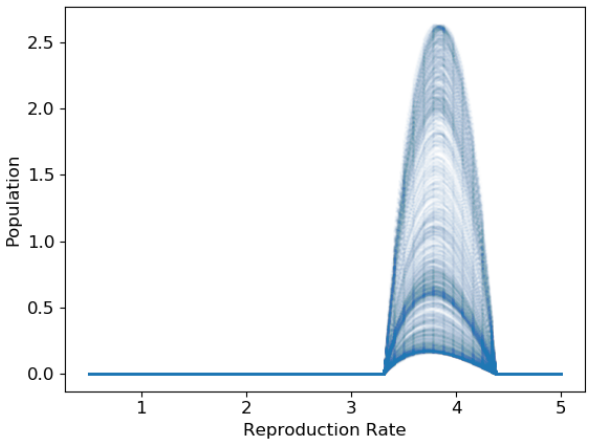

Fig. 9. Bifurcation map of 500 individual populations with reproduce rates linearly spaced from 0.5-5.0. All populations are initialized to the same initial population of 1.0. 10,000 transient populations pass before collecting 1000 generations for the bifurcation map.

reproductive rates. Then for higher maximum rate the steady state population oscillates together between various population levels. For the maximum reproductive rate of 3.33, whose time series is also displayed in figure 8, the populations oscillate between two states. Then for the maximum displayed reproductive rate of 4.00, it oscillates between 8 equilibrium points. For the maximum reproductive rate of 4.00, there are four points readily observable in figure 7, which are actually two very closely spaced points, for a total of 8. We see that much of the underlying characteristics of the logistic map are preserved. This shows that with increasing reproductive rates, the population goes from a single to a double, to a multi-level attractor, up until the population become chaotic. In figure 9, the bifurcation map for 500 coupled populations with linearly spaced reproductive coefficients from $r = 0.5$ to $r = 5.0$ is shown. The plot is a scatter plot of 1000 steady state generations after 10,000 transient populations have passed. We see that there is a preferred range of reproductive rates that are supported by the system. Furthermore, within that band of supported populations there are three darker region around 2.5, 0.5,and 0.25. The darker the region, the more often the system has been in that state over the recorded 1000 states. Otherwise the populations tend cover the entire region. The surviving populations do not oscillate between fixed states, however successive generations follow a distinctive patter as illustrated in 10. This figure shows a scatter plot of current generations, vs the next generation at each step.The left figure is the total population, which shows a clear mapping from one population to the next. Similarly for each individual population on the right there is also a clear mapping between one generations to the next. For each individual population, it is important to note the width of the mappings in comparison to the width of the total population curve. From a qualitative stand point this can be thought of as a measure of uncertainty.

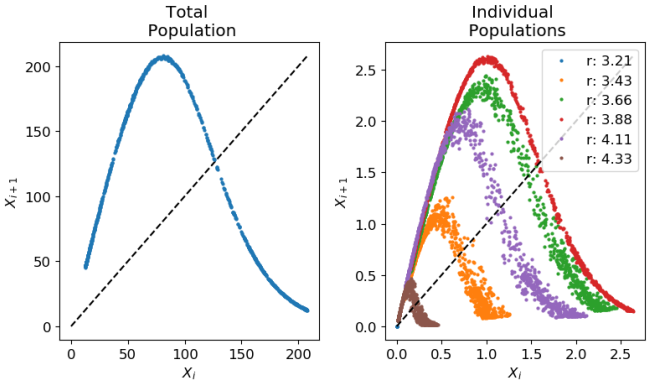

Fig. 10. Scatter plot of current populations X_i, to the proceeding population X_{i+1} for the total population (left), and individual populations (right).

For instance, consider that the current total population is 150, from the total population curve (figure 10, left), this would indicate the next generation will have a total population of 70. However if we consider the individual population (figure 10, right) with reproductive rate of $r = 3.43$ with a current population of 1, this maps to 0.1 to 0.6. To further illustrate this consider figure 11. In this plot the time series of the total population is normalized between 0 and 1. Similarly the population with the reproductive rate of $r = 3.80$, the population that has the peak individual population in figure 9. And two other populations are also normalized between zero and one. The following figure shows that the smaller populations do not closely track the total population, in comparison to the maximum population.

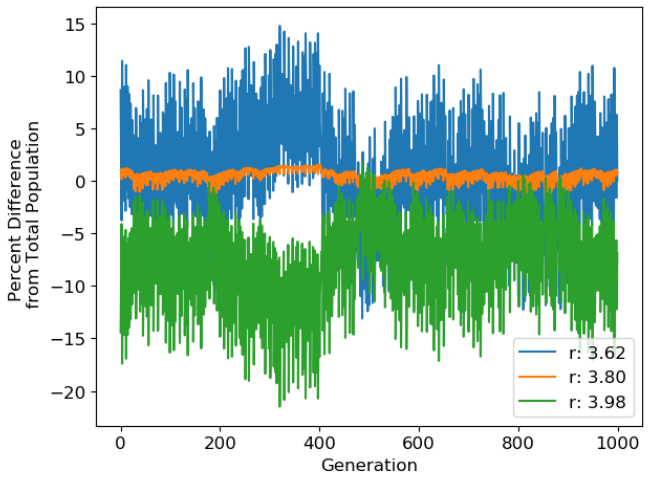

Fig. 11. Comparison of individual populations to the total populations. For each individual population and the total population the time series are mapped from zero to 1. Then at each generation the percent difference between individual and total population is calculated.

There is still considerable analysis to be done to fully understand the relationship between the individual populations and the total populations. We have also seen that for increasing maximum reproductive rates (0.5-10) multiple isolated regions of reproductive rates are supported. At this point significant time was dedicated to understating the basic dynamics of this system. In the future we would be investigating the mutual information and transfer entropy between the total population and individual populations at the peak, and the wings of the supported populations.

III. Discussion and Conclusions

For the most part our results were qualitatively and quantitatively in agreement with those seen in the Walker paper. The switch from bottom-up driven to top-down driven causal information transfer for global coupling strength $\epsilon > 0.2$ is mostly consistent, alongside the emergence of sub-communities forming in the return map for coupling strengths with dominant top-down information transfer. One discrepancy noted is the response that Walker shows for $\epsilon = 0.075$, which seems to not be driven by top-down information transfer at all as previously concluded [1].

References

[1] S. I. Walker, L. Cisneros, P.C.W. Davies, “Evolutionary Transitions and Top-Down Causation,” Artificial Life 13, Feb. 2012.

[2] M. Mitchell, Complexity: a guided tour. Oxford: Oxford University Press, 2011.

[3] T. Schreiber, ”Measuring Information Transfer”, Physical Review Letters, vol. 85, no. 2, pp. 461-464, 2000. Available: 10.1103/physrevlett.85.461.

[4] J. T. Lizier, ”JIDT: An information-theoretic toolkit for studying the dynamics of complex systems”, Frontiers in Robotics and AI 1:11, 2014; doi:10.3389/frobt.2014.00011 (pre-print: arXiv:1408.3270)

[5] G. Flake, ”The Computational Beauty of Nature”, Cambridge, Mass.: The MIT press, 2011, pp. 139-151.

IV. Contributions

Work done on this project was very evenly distributed between the two group members. Justin provided the results, analysis and write-up of part A and part D, while Catherine provided the results, analysis and write-up of part B and part C. Both team members took part in writing the abstract, introduction, and conclusions. All code used in this project was written by Justin and Catherine, except for code generated by JIDT tool [4], which is commented as such in our programs.

The source code for all results generated in this project can be found at https://github.com/judeter/CS523-TopDownCausation